

THE UNIVERSITY OF MICHIGAN
INDUSTRY PROGRAM OF THE COLLEGE OF ENGINEERING

A STUDY TO DETERMINE THE INELASTIC MOMENT-CURVATURE
RELATION OF STRUCTURAL MEMBERS

M. J. Kaldjian

October, 1966

IP-753

TABLE OF CONTENTS

	<u>Page</u>
LIST OF TABLES.....	iii
LIST OF FIGURES.....	iv
INTRODUCTION.....	1
ASSUMPTIONS.....	4
RESULTANT FORCE AND MOMENT.....	7
STRESS CENTER (CENTER OF PRESSURE).....	9
WIDE-FLANGE SECTIONS.....	10
NUMERICAL WORK.....	16
SIMPLIFIED EXPRESSIONS.....	16
ALTERNATE EXPRESSION.....	22
DISCUSSION OF RESULTS.....	23
CONCLUSIONS.....	23
REFERENCES.....	25
ACKNOWLEDGEMENTS.....	25
APPENDIX - NOTATIONS.....	26

LIST OF TABLES

<u>Table</u>		<u>Page</u>
I	APPROXIMATED SECTION PROPERTIES.....	10
II	MOMENT-CURVATURE PARAMETERS COMPARED FOR $r = 10$, $\sigma_y = 36$ ksi, $\epsilon_y = .0012$ in/in, $\mu = 10$	17
III	MOMENT-CURVATURE PARAMETERS COMPARED FOR $r = 10$, $\sigma_y = 36$ ksi, $\epsilon_y = .0012$ in/in, $\mu = 5$	18
IV	MOMENT-CURVATURE PARAMETERS COMPARED FOR $r = 10$, $\sigma_y = 36$ ksi, $\epsilon_y = .0012$ in/in, $\mu = 20$	19
V	MOMENT-CURVATURE PARAMETERS COMPARED FOR $r = 5$, $\sigma_y = 36$ ksi, $\epsilon_y = .0012$ in/in, $\mu = 10$	20

LIST OF FIGURES

<u>Figure</u>	<u>Page</u>
1. Ramberg-Osgood Functions.....	2
2. Ramberg-Osgood Load-displacement Relations.....	2
3. Experimental Hysteresis Loops.....	3
4. Stress-strain Relation.....	6
5. Stress and Strain Distribution Across Section.....	6
6. Wide-Flange Section Approximation.....	6
7. Moment-curvature Relation For 21WF62 ($\sigma_y = 36$, $\epsilon_y = .0012$ and $\mu = 10$).....	12
8. Simplified Moment-curvature Expressions Compared For 21WF62 ($\sigma_y = 36$, $\epsilon_y = .0012$ and $\mu = 10$).....	13
9. Moment-curvature Relation For 21WF62 ($\sigma_y = 36$, $\epsilon_y = .0012$ and $\mu = 10$).....	14
10. Simplified Moment-curvature Expressions Compared for 21WF62 ($\sigma_y = 36$, $\epsilon_y = .0012$ and $\mu = 10$).....	15

INTRODUCTION

Experimental work has shown that the load-displacement (or moment-curvature) relationship for structural members, structural steel in particular, is not an elasto-plastic curve. The actual load displacement curve has an elastic branch followed by a transition curve that leads to a plastic branch⁽¹⁾. When the displacement is reversed, due to Bauschinger effect, the transition becomes more gradual. Such a relationship can be expressed quite closely by a Ramberg-Osgood function,^{(2),(3),(4)}

$$\frac{x}{x_y} = \frac{q}{q_y} \left(1 + \left| \frac{q}{q_y} \right|^{r-1} \right) \quad (1)$$

where x = the displacement (or curvature)

x_y = a characteristic displacement

q = the load (or moment)

q_y = a characteristic load

r = an exponent

x_y , q_y and r are the Ramberg-Osgood parameters.

Plots of Equation (1) are shown in Figure 1 for various values of r . It also includes as limiting cases the elastic ($r=1$) and the elasto-plastic ($r = \infty$) relations. A complete description of a Ramberg-Osgood equation is found in Figure 2.

Ramberg-Osgood parameters so far have been determined from test results only. Data for a given section are obtained in the form of load-displacement (moment-curvature) hysteresis loops and the parameters q_y , x_y and r are chosen to give the best fit in the sense of least squares. A typical example of this is shown in Figure 3.⁽²⁾

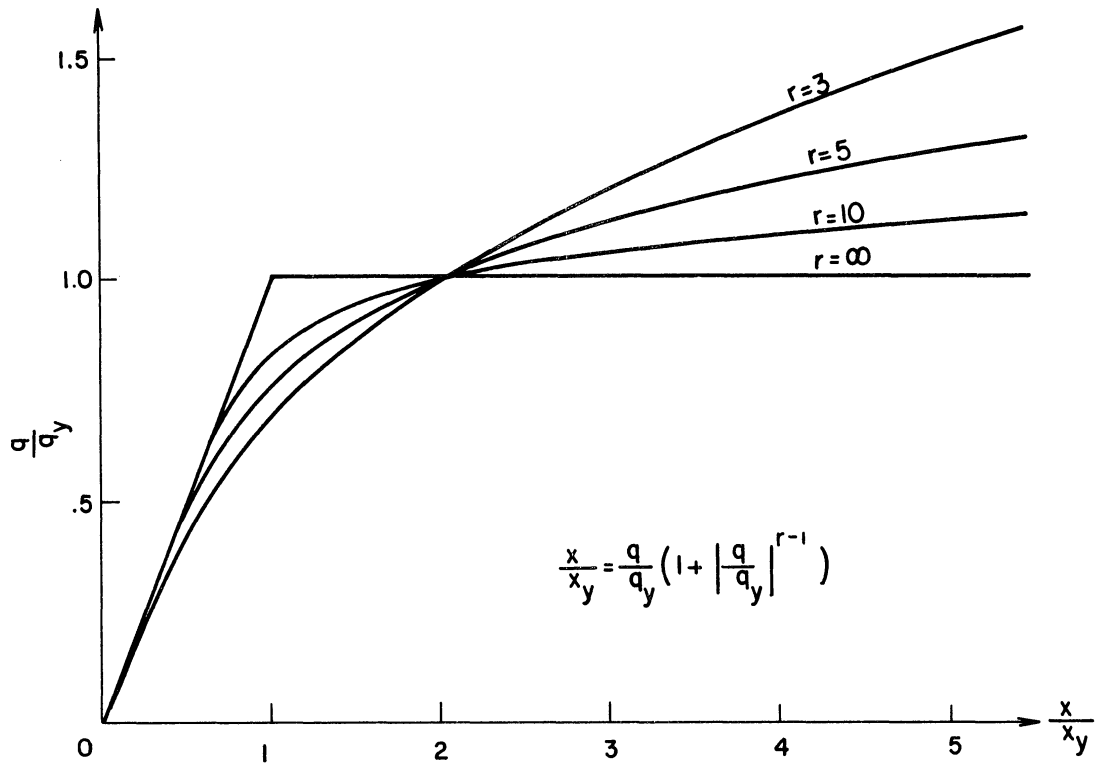


Figure 1. Ramberg-Osgood Functions.

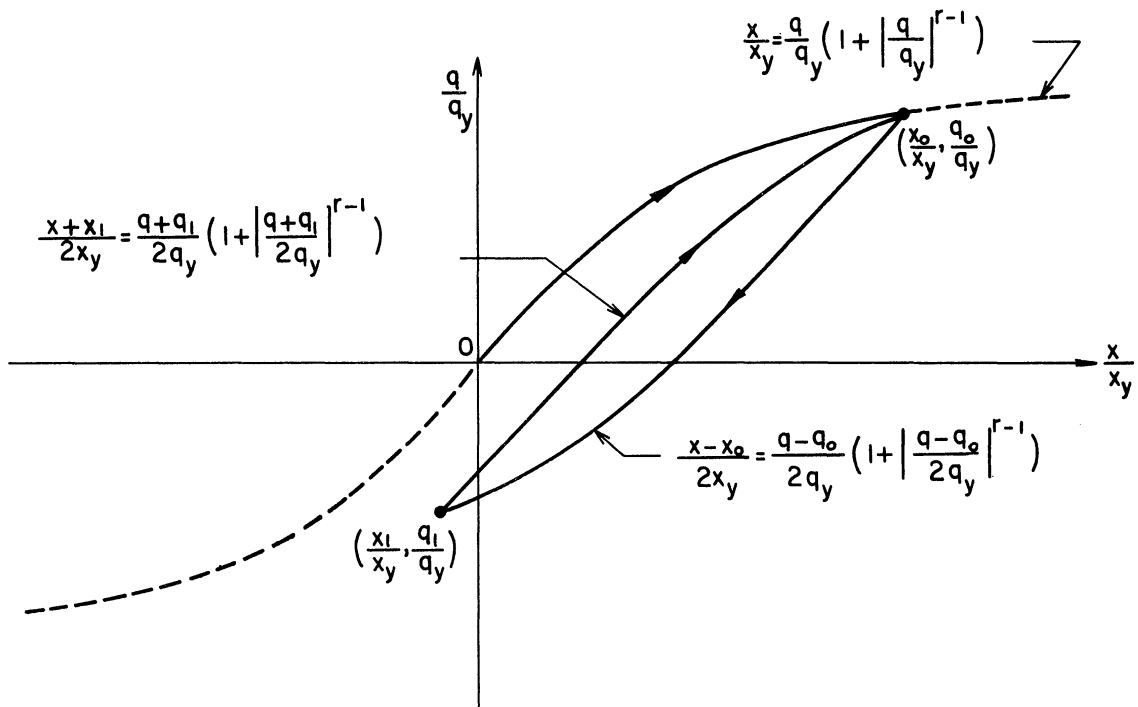


Figure 2. Ramberg-Osgood Load-displacement Relations.

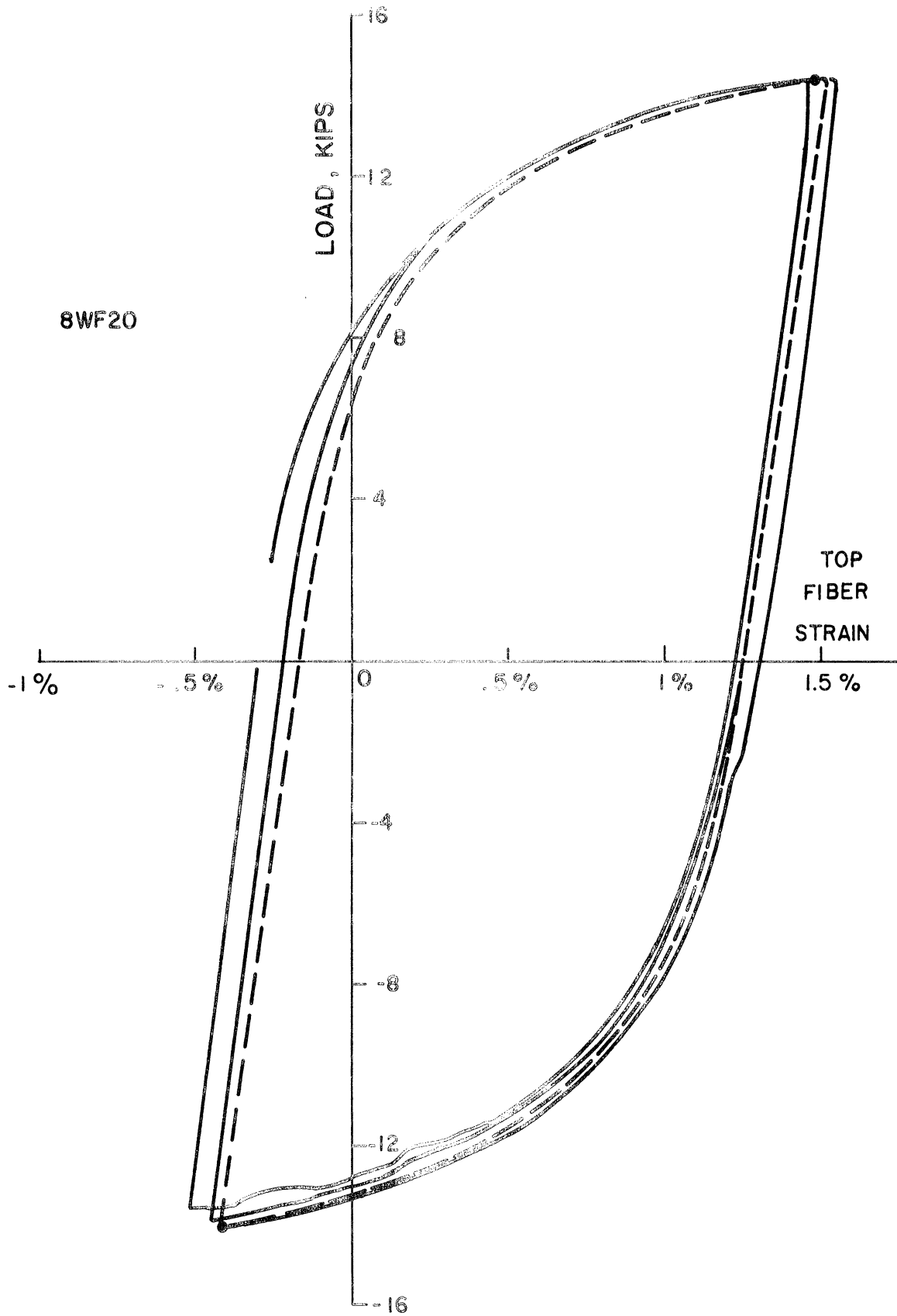


Figure 3. Experimental Hysteresis Loops.

The purpose of the present study is to find an analytical basis to determine these parameters for various sections

- a) from a stress-strain consideration, when the stress-strain relation across a section in bending can be expressed by a Ramberg-Osgood function⁽⁵⁾.
- b) when a set of parameters for a section is available, say from experimental results.

Finding the Ramberg-Osgood parameter is essential in seismic design. Dynamic analysis of a multi-degree-of-freedom structural frame can be performed only after the parameters x_y , q_y and r are known for all the members in the frame.

ASSUMPTIONS

To develop moment-curvature relations, the following assumptions are being made:

- a. Beams are prismatic and straight, and have a cross-sectional area of symmetry about the plane of bending.
- b. Planes normal to the axis of the beam remain plane after deformation, i.e., strains vary linearly from the neutral axis.
- c. The stress-strain relation is of the Ramberg-Osgood type and is applicable to the individual fibers in tension as well as in compression.
- d. A wide-flange section can be closely approximated by the difference of two rectangles.

From assumption (c), the stress-strain relation is given as

$$\frac{\epsilon}{\epsilon_y} = \frac{\sigma}{\sigma_y} \left(1 + \left| \frac{\sigma}{\sigma_y} \right|^{r-1} \right) \quad (2)$$

where ϵ = the strain

σ = the stress

ϵ_y = a characteristic strain

σ_y = a characteristic stress

r = an exponent

ϵ_y , σ_y and r are the Ramberg-Osgood stress-strain parameters, and can be determined from test results.

For a given bending moment M at a section along a beam let the maximum stress and the maximum strain in the extreme fibers be represented by σ_m and ϵ_m respectively, see Figure 4. The stress and the strain distribution across the section is shown in Figure 5. The stress at any point y from the neutral axis (Figure 5) can be expressed as

$$\sigma = \sigma_m - x_\sigma$$

where x_σ is the difference between the stress at the extreme fiber and the stress at point y . The corresponding expression for strain from Equation (2) becomes

$$\epsilon = \epsilon_y \left[\left(\frac{\sigma_m - x_\sigma}{\sigma_y} \right) \left(1 + \left| \frac{\sigma_m - x_\sigma}{\sigma_y} \right|^{r-1} \right) \right] \quad (3a)$$

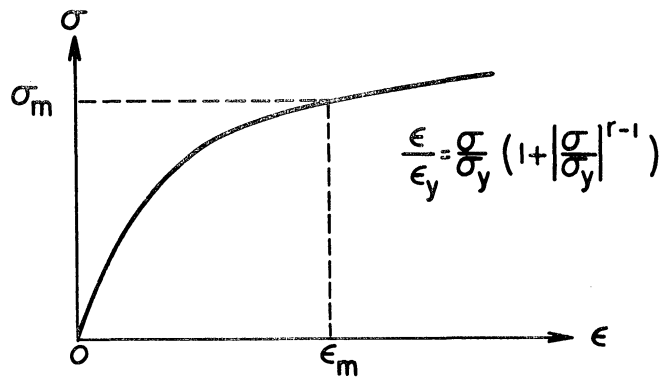


Figure 4. Stress-strain Relation.

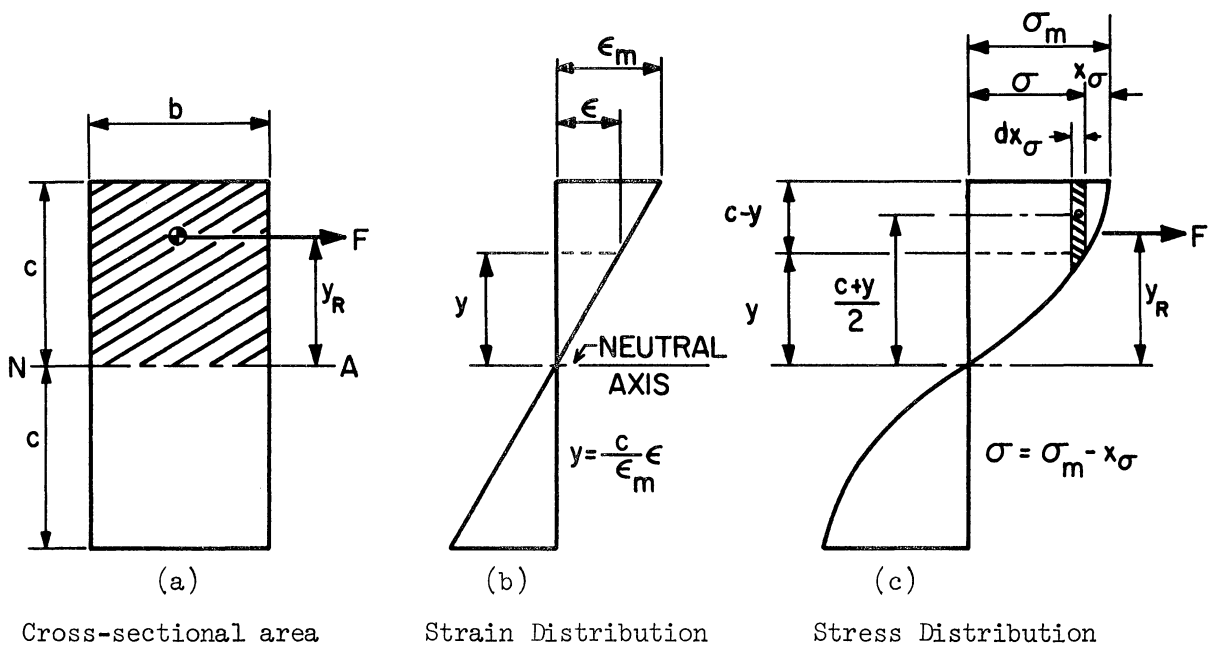


Figure 5. Stress and Strain Distribution Across Section.

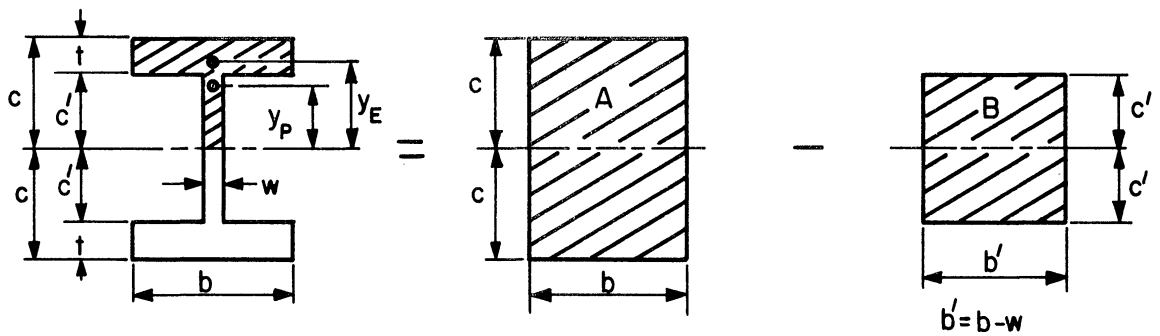


Figure 6. Wide-Flange Section Approximation.

At the extreme fiber the strain

$$\epsilon_m = \epsilon_y \left[\left(\frac{\sigma_m}{\sigma_y} \right) \left(1 + \left| \frac{\sigma_m}{\sigma_y} \right|^{r-1} \right) \right] \quad (3b)$$

RESULTANT FORCE AND MOMENT

For a rectangular cross-section of width b and depth $2c$ the differential element of force dF and moment dM from Figure 5 are

$$dF = b(c - y) dx_\sigma \quad (4)$$

and

$$dM = \frac{c + y}{2} dF = \frac{b}{2} (c^2 - y^2) dx_\sigma \quad (5)$$

also from Figure 5

$$y = \frac{c}{\epsilon_m} \epsilon \quad (6)$$

Substituting Equations (3a), (3b) and (6) into Equations (4) and (5) and simplifying, results in

$$dF = bc \left\{ 1 - \frac{1}{\mu} \left[\frac{\sigma_m - x_\sigma}{\sigma_y} + \left(\frac{\sigma_m - x_\sigma}{\sigma_y} \right)^r \right] \right\} dx_\sigma \quad (7)$$

and

$$dM = \frac{bc^2}{2} \left\{ 1 - \frac{1}{\mu^2} \left[\frac{\sigma_m - x_\sigma}{\sigma_y} + \left(\frac{\sigma_m - x_\sigma}{\sigma_y} \right)^r \right]^2 \right\} dx_\sigma \quad (8)$$

where

$$\mu = \frac{\epsilon_m}{\epsilon_y} = \frac{\sigma_m}{\sigma_y} + \left(\frac{\sigma_m}{\sigma_y} \right)^r = \text{the ductility ratio.}$$

Note that the absolute value notations in Equations (7) and (8) have been left out because $(\sigma_m - x_\sigma)/\sigma_y$ in this analysis is always positive.

The resultant force F over half the section, i.e., to one side of the neutral axis, is obtained by integrating Equation (7) from $x_\sigma = 0$ to $x_\sigma = \sigma_m$:

$$F = \int_0^{\sigma_m} bc \left\{ 1 - \frac{1}{\mu} \left[\frac{\sigma_m - x_\sigma}{\sigma_y} + \left(\frac{\sigma_m - x_\sigma}{\sigma_y} \right)^r \right] \right\} dx_\sigma$$

Performing the integration over the limits, the resultant force becomes

$$F = \sigma_m bc \left\{ 1 - \frac{1}{2\mu} \left[\frac{\sigma_m}{\sigma_y} + \frac{2}{r+1} \left(\frac{\sigma_m}{\sigma_y} \right)^{r+1} \right] \right\} \quad (9)$$

To obtain the total moment M , Equation (8) is integrated over the whole section, thus,

$$M = bc^2 \int_0^{\sigma_m} \left\{ 1 - \frac{1}{\mu^2} \left[\frac{\sigma_m - x_\sigma}{\sigma_y} + \left(\frac{\sigma_m - x_\sigma}{\sigma_y} \right)^r \right]^2 \right\} dx_\sigma$$

which, upon integrating and simplifying, reduces to

$$M = \sigma_m bc^2 \left\{ 1 - \frac{1}{\mu^2} \left[\frac{1}{3} \left(\frac{\sigma_m}{\sigma_y} \right)^2 + \frac{2}{r+2} \left(\frac{\sigma_m}{\sigma_y} \right)^{r+1} + \frac{1}{2r+1} \left(\frac{\sigma_m}{\sigma_y} \right)^{2r} \right] \right\} \quad (10)$$

The curvature ϕ corresponding to the moment above is obtained by dividing the extreme fiber strain ϵ_m by its distance from the neutral axis.

In equation form the curvature

$$\phi = \frac{\epsilon_m}{c} = \frac{\epsilon_y}{c} \left[\frac{\sigma_m}{\sigma_y} + \left(\frac{\sigma_m}{\sigma_y} \right)^r \right] \quad (11)$$

STRESS CENTER (CENTER OF PRESSURE)

The stress center y_R for a rectangular section is found by taking half the total moment and dividing it by the resultant force, i.e.,

$$y_R = \frac{M}{2F}$$

Substituting Equations (9) and (10) into above and simplifying, yields the desired expression for the stress center

$$y_R = \frac{c}{2} \frac{1 - \frac{1}{3\mu} \left(z_m^2 + \frac{6}{r+2} z_m^{r+1} + \frac{3}{2r+1} z_m^{2r} \right)}{1 - \frac{1}{2\mu} \left(z_m + \frac{2}{r+1} z_m^r \right)} \quad (12)$$

where

$$z_m = \frac{\sigma_m}{\sigma_y}$$

When the section approaches the fully plastic condition of stress, the ductility ratio μ tends to infinity making the stress center y_R in Equation (12) approach $c/2$. On the other hand, a fully elastic distribution of stress in the section reduces y_R to $\frac{2}{3}c$. These are to be expected for rectangular sections as limiting values for y_R . The stress center for any section must therefore lie between

$$y_P \leq y_R \leq y_E$$

where y_P = the stress center for the fully plastic case

and y_E = the stress center for the fully elastic case.

TABLE I
APPROXIMATED SECTION PROPERTIES

Section	Area	Sec. Mod. S_x	Plas. Mod. Z_x	y_p	y_E
4 LC 13	3.765 (3.82)	5.225 (5.2)	6.012 (6.1)	1.597	1.738
3WF 17	4.932 (5.00)	13.895 (14.1)	15.573 (15.8)	3.157 (3.16)	3.569 (3.566)
8 WF 20	5.814 (5.88)	16.795 (17.0)	18.837 (19.1)	3.240 (3.24)	3.629 (3.626)
10 WF 25	7.279 (7.35)	26.170 (26.4)	29.265 (29.5)	4.021 (4.02)	4.507 (4.503)
12 WF 36	10.494 (10.59)	45.448 (45.9)	50.974 (51.4)	4.857 (4.86)	5.457 (5.455)
16 WF 50	14.581 (14.70)	79.883 (80.7)	90.748 (92.7)	6.224 (6.24)	7.152 (7.16)
21 WF 62	18.039 (18.23)	124.76 (126.4)	142.30 (144.1)	7.888 (7.90)	9.202 (9.20)
24 WF 84	24.516 (24.71)	194.41 (196.3)	222.01 (224.0)	9.056 (9.07)	10.547 (10.55)
30 WF 108	31.444 (31.77)	295.12 (299.2)	341.27 (345.5)	10.853 (10.88)	12.894 (12.90)
8 x 4	32.00	42.667	64.00	2.00	2.667

NOTE: Bracketed numbers are from actual sections for comparison.

WIDE-FLANGE SECTIONS

A wide-flange section can be closely approximated by the difference of two rectangles as shown in Figure 6.

The moment M_{WF} in a wide-flange section can be given as

$$M_{WF} = M_A - M_B \quad (13)$$

The subscripts A and B refer respectively to rectangles A and B in Figure 6.

For a given σ_m in the extreme fiber of wide flange M_A , the moment in rectangle A, is found explicitly from Equation (10). There is, however, no direct way of obtaining M_B . To find the latter, the fiber strain at c' (i.e., $\frac{c'}{c} \epsilon_m$) in Figure 6 is first calculated and the corresponding stress is found from Equation (2) by a numerical method. This is the extreme fiber stress in rectangle B and is used in Equation (10) to obtain the value of M_B . With M_A and M_B known the moment M_{WF} in the wide-flange section is determined from Equation (13), and the curvature ϕ , corresponding to M_{WF} , is obtained from Equation (11).

MOMENT-CURVATURE PARAMETERS

Points along the moment-curvature plot for a wide-flange section are calculated from Equations (10), (11) and (13) by varying the extreme fiber stress σ_m , and the moment-curvature parameters M_y (a characteristic moment), ϕ_y (a characteristic curvature) and R (an exponent) are chosen to give the best fit in the sense of least squares. Fitting the curve through the points is done with the aid of a computer.

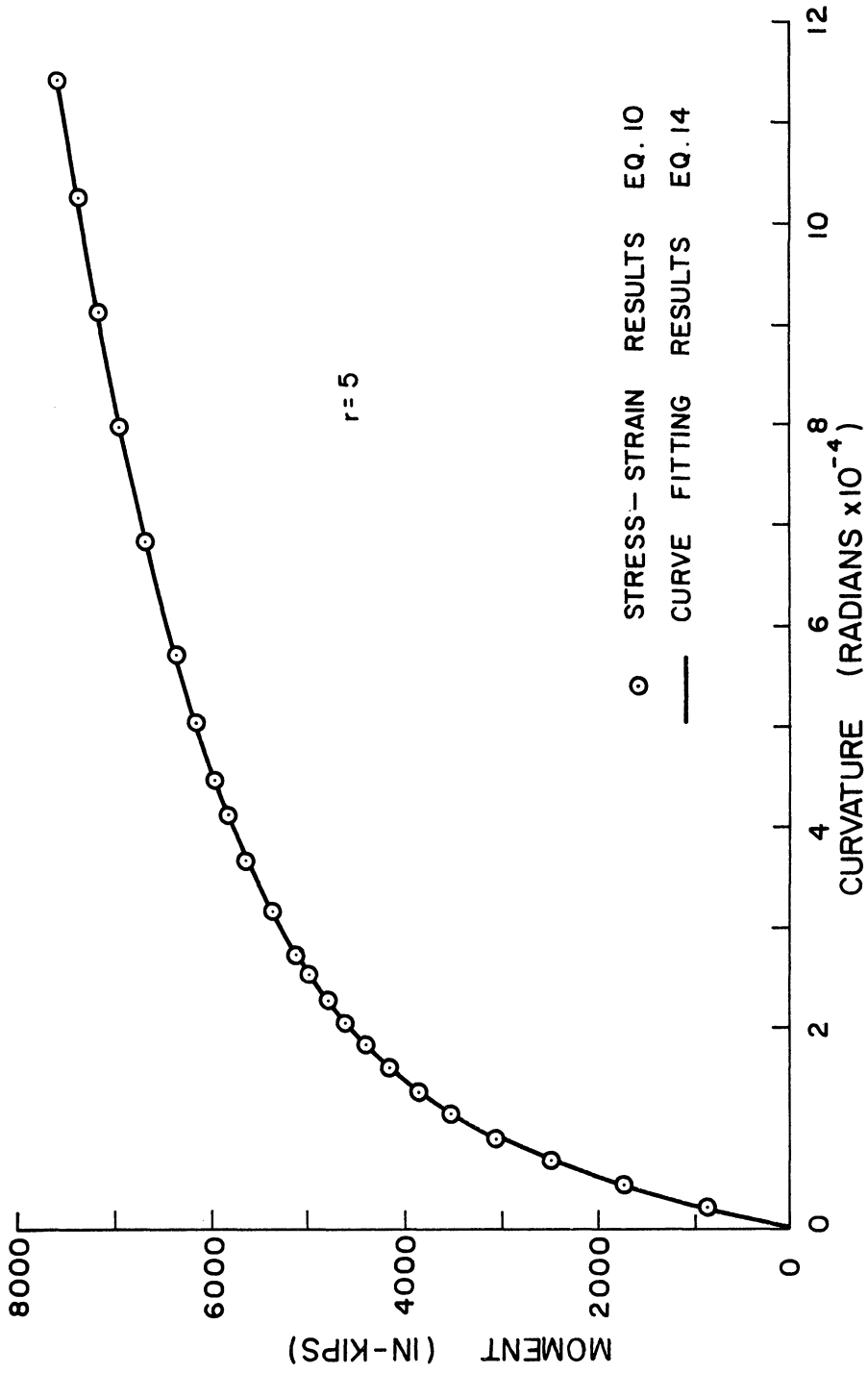


Figure 7. Moment-curvature Relation For 21WF62 ($\sigma_y = 36$, $\epsilon_y = .0012$ and $\mu = 10$).

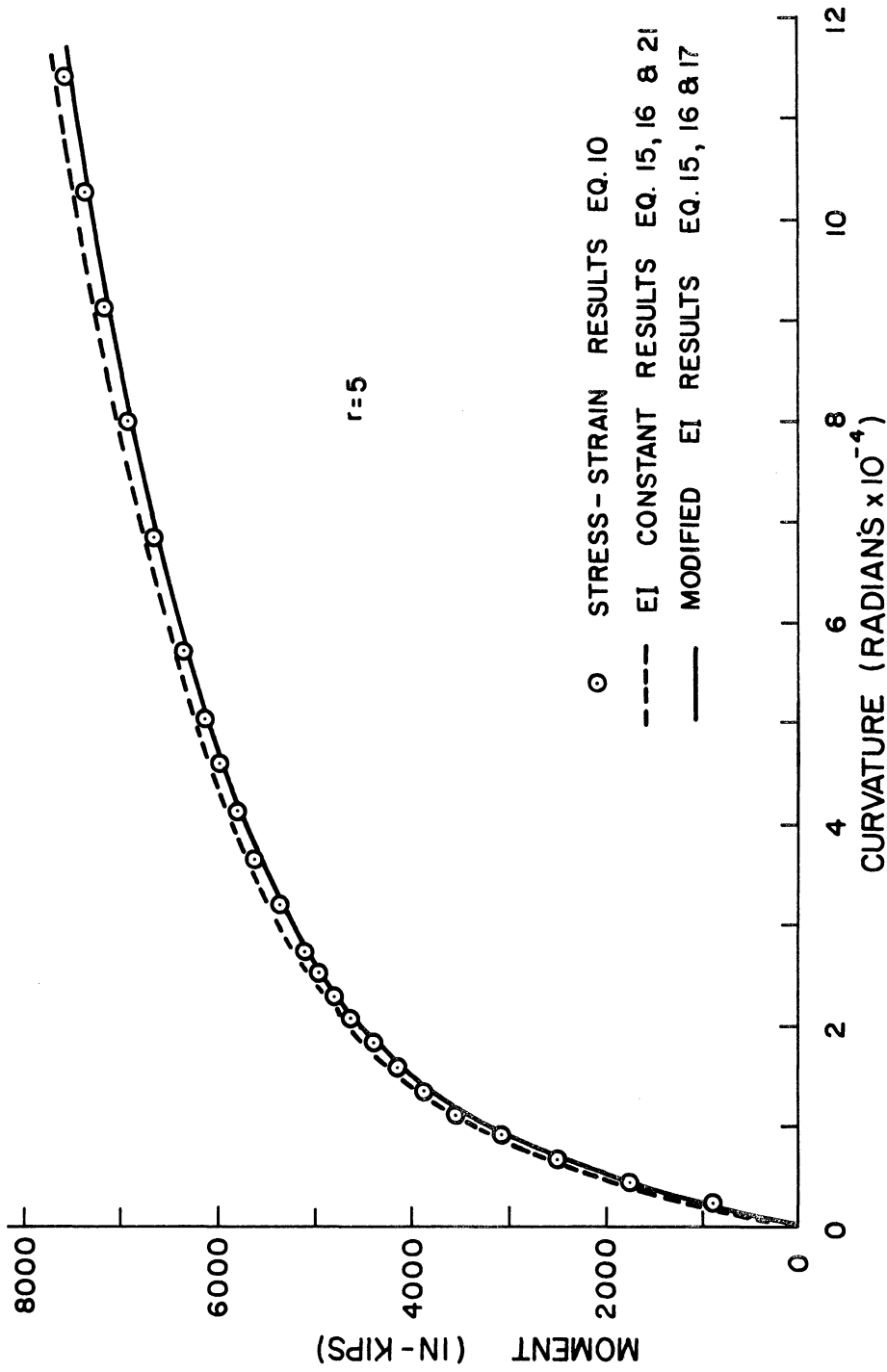


Figure 8. Simplified Moment-curvature Expressions Compared
For 21WF62 ($\sigma_y = 36$, $\epsilon_y = .0012$ and $\mu = 10$).

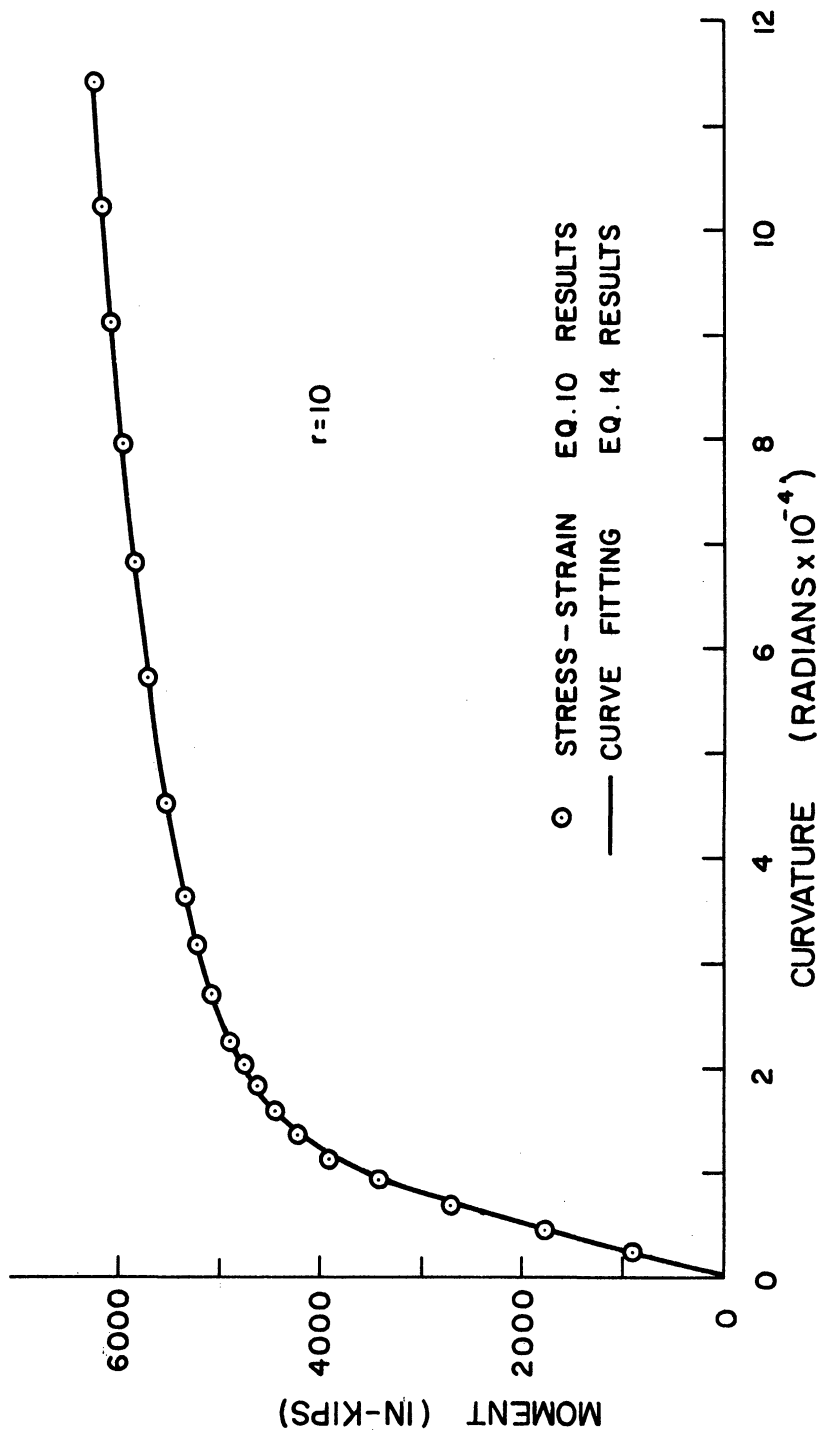


Figure 9. Moment-curvature Relation For 21WF62 ($\sigma_y = 36$, $\epsilon_y = .0012$ and $\mu = 10$).

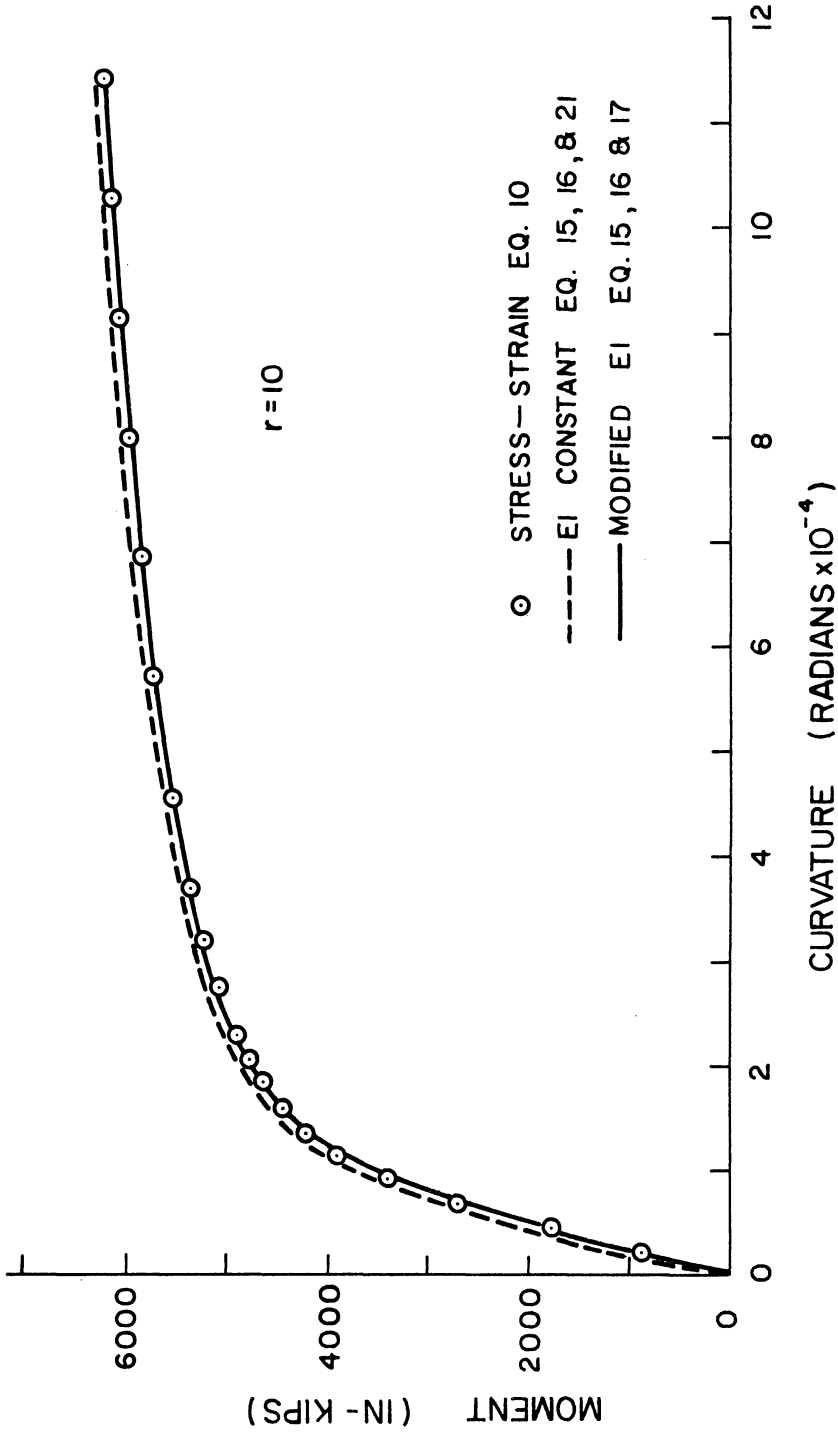


Figure 10. Simplified Moment-curvature Expressions Compared for 2LWF62 ($\sigma_y = 36$, $\epsilon_y = .0012$ and $\mu = 10$).

Thus, a single relation between moment and curvature is established:

$$\frac{\phi}{\phi_y} = \frac{M}{M_y} \left(1 + \left| \frac{M}{M_y} \right|^{R-1} \right) \quad (14)$$

Moment-curvature plots from stress consideration as well as from curve fitting Equation (14) are shown plotted in Figures 7 and 9 for 21 WF 62. The results are typical for the wide-flange sections considered.

NUMERICAL WORK

To test the preceding presentation numerically, nine structural steel sections are chosen ranging from 4 LC 13 to 30 WF 108. Also a rectangular section 8" x 4" is considered for comparison.

To obtain the moment-curvature parameters, a stress-strain curve of the Ramberg-Osgood type and a ductility ratio are assumed. Points along the moment-curvature plot are calculated for each section from Equations (10), (11) and (13), and the parameters M_y , ϕ_y and R for Equation (14) are chosen.

Moment-curvature parameters are determined for various stress-strain parameters and ductility ratios, and are shown tabulated in Tables II through V.

SIMPLIFIED EXPRESSIONS

To obtain the moment-curvature parameters the need for simplicity is apparent. The following simplified relations are being proposed for wide-flange sections:

- a) When the stress-strain parameters (ϵ_y , σ_y and r) are known,

TABLE II
MOMENT-CURVATURE PARAMETERS COMPARED FOR

$$r = 10, \sigma_y = 36 \text{ ksi}, \epsilon_y = .0012 \text{ in/in}$$

$$\mu = 10$$

Section	R	M_y (in-kips)	$\phi_y \times 10^4$ (radians)	$\frac{M_y}{\phi_y} \times 10^{-4}$	$EI \times 10^{-4}$ (kip-in ²)
4 LC 13	9.845	216.11	7.192	30.05	31.35
	(10.0)	(216.43)	(7.196)	(30.08)	
	<u>9.715</u>	<u>215.82</u>	<u>7.205</u>	<u>29.95</u>	
8 WF 17	9.779	559.49	3.570	156.72	166.74
	(10.0)	(560.63)	(3.568)	(157.12)	
	<u>9.715</u>	<u>559.04</u>	<u>3.572</u>	<u>156.50</u>	
8 WF 20	9.796	676.85	3.494	193.71	205.07
	(10.0)	(678.13)	(3.494)	(194.08)	
	<u>9.715</u>	<u>676.21</u>	<u>3.498</u>	<u>193.31</u>	
10 WF 25	9.795	1051.57	2.815	373.55	395.69
	(10.0)	(1053.5)	(2.814)	(374.37)	
	<u>9.715</u>	<u>1050.56</u>	<u>2.818</u>	<u>372.80</u>	
12 WF 36	9.790	1831.5	2.327	787.06	834.43
	(10.0)	(1835.1)	(2.327)	(788.61)	
	<u>9.715</u>	<u>1829.9</u>	<u>2.330</u>	<u>785.36</u>	
16 WF 50	9.744	3258.8	1.795	1815.48	1947.15
	(10.0)	(3266.9)	(1.794)	(1821.01)	
	<u>9.715</u>	<u>3257.7</u>	<u>1.796</u>	<u>1813.86</u>	
21 WF 62	9.715	5108.3	1.406	3633.21	3928.07
	(10.0)	(5122.7)	(1.404)	(3648.64)	
	<u>9.715</u>	<u>5108.3</u>	<u>1.406</u>	<u>3633.21</u>	
24 WF 84	9.717	7969.9	1.225	6506.04	7025.0
	(10.0)	(7992.4)	(1.224)	(6529.73)	
	<u>9.715</u>	<u>7969.7</u>	<u>1.226</u>	<u>6500.57</u>	
30 WF 108	9.674	12244	1.012	12098.8	13245.0
	(10.0)	(12286)	(1.011)	(12152.8)	
	<u>9.715</u>	<u>12251</u>	<u>1.012</u>	<u>12105.7</u>	
8 x 4	9.210	2272.4	5.032	451.59	512.00
	(10.0)	(2304.0)	(5.142)	(448.07)	
	<u>9.715</u>	<u>2297.5</u>	<u>5.149</u>	<u>446.20</u>	

NOTE: Bracketed numbers are derived from Equations 15, 16 and 17. Underlined numbers are from Equations 18, 19 and 20 based on Section 21 WF 62 values.

TABLE III

MOMENT-CURVATURE PARAMETERS COMPARED FOR

$$r = 10, \sigma_y = 36 \text{ ksi}, \epsilon_y = .0012 \text{ in/in}$$

$$\mu = 5$$

Section	R	M_y (in-kips)	$\phi_y \times 10^4$ (radians)	$\frac{M_y}{\phi_y} \times 10^{-4}$	$EI \times 10^{-4}$ (kip-in ²)
4 LC 13	9.577	214.51	6.948	30.87	31.35
	(10.0)	(216.43)	(6.904)	(31.35)	
	9.231	212.82	6.983	30.48	

8 WF 20	9.442	669.98	3.333	201.01	205.07
	(10.0)	(678.13)	(3.307)	(205.06)	
	9.231	666.81	3.345	199.35	

21 WF 62	9.231	5037.3	1.319	3819.0	3928.07
	(10.0)	(5122.7)	(1.304)	(3928.5)	
	9.231	5037.3	1.319	3819.0	

30 WF 108	9.130	120533	.943	12782	13245.0
	(10.0)	(12286)	(.931)	(13197)	
	9.231	12081	.941	12838	

8 x 4	8.183	2215.3	4.526	489.5	512.00
	(10.0)	(2304.0)	(4.500)	(512.0)	
	9.231	2266	4.552	497.8	

NOTE: Bracketed numbers are derived from Equations 15, 16 and 17a.
Underlined numbers are from Equations 18, 19 and 20a based on Section 21 WF 62 values.

TABLE IV

MOMENT-CURVATURE PARAMETERS COMPARED FOR
 $r = 10$, $\sigma_y = 36$ ksi, $\epsilon_y = .0012$ in/in

$\mu = 20$

Section	R	M_y (in-kips)	$\phi_y \times 10^4$ (radians)	$\frac{M_y}{\phi_y} \times 10^{-4}$	$EI \times 10^{-4}$ (kip-in ²)
4 LC 13	9.967	217.39	7.422	29.29	31.35
	(10.0)	(216.43)	(7.52)	(28.78)	
	<u>9.937</u>	<u>218.10</u>	<u>7.340</u>	<u>29.71</u>	
8 WF 20	9.956	682.14	3.644	187.20	205.07
	(10.0)	(678.13)	(3.71)	(182.78)	
	<u>9.937</u>	<u>683.35</u>	<u>3.618</u>	<u>188.88</u>	
21 WF 62	9.937	5162.2	1.486	3473.9	3928.07
	(10.0)	(5122.7)	(1.522)	(3365.8)	
	<u>9.937</u>	<u>5162.2</u>	<u>1.486</u>	<u>3473.9</u>	
30 WF 108	9.926	12388	1.076	11513	13245.0
	(10.0)	(12286)	(1.105)	(11119)	
	<u>9.937</u>	<u>12380</u>	<u>1.080</u>	<u>11463</u>	
8 x 4	9.771	2321.4	5.570	416.8	512.00
	(10.0)	(2304.0)	(6.00)	(384.0)	
	<u>9.937</u>	<u>2321.7</u>	<u>5.861</u>	<u>396.1</u>	

NOTE: Bracketed numbers are derived from Equations 15, 16 and 17b.
 Underlined numbers are from Equation 18, 19 and 20b based on
 Section 21 WF 62 values.

TABLE V
 MOMENT-CURVATURE PARAMETERS COMPARED FOR
 $r = 5, \sigma_y = 36 \text{ ksi}, \epsilon_y = .0012 \text{ in/in}$

$\mu = 10$

Section	R	M_y (in-kips)	$\phi_y \times 10^4$ (radians)	$\frac{M_y}{\phi_y} \times 10^{-4}$	$EI \times 10^{-4}$ (kip-in ²)
4 LC 13	4.966	215.45	6.992	30.81	31.35
	(5.0)	(216.43)	(7.196)	30.08	
	<u>4.937</u>	<u>214.61</u>	<u>6.841</u>	<u>31.37</u>	
8 WF 20	4.955	674.05	3.363	200.43	205.07
	(5.0)	(678.13)	(3.494)	(194.08)	
	<u>4.937</u>	<u>672.41</u>	<u>3.321</u>	<u>202.47</u>	
21 WF 62	4.937	5079.6	1.335	3805.0	3928.07
	(5.0)	(5122.7)	(1.404)	(3648.6)	
	<u>4.937</u>	<u>5079.6</u>	<u>1.335</u>	<u>3805.0</u>	
30 WF 108	4.928	12167	.956	12727	13245.0
	(5.0)	(12286)	(1.011)	(12152)	
	<u>4.937</u>	<u>12182</u>	<u>.961</u>	<u>12676</u>	
8 x 4	4.828	2249.8	4.664	482.4	512.00
	(5.0)	(2304.0)	(5.142)	(448.1)	
	<u>4.937</u>	<u>2284.6</u>	<u>4.889</u>	<u>467.3</u>	

NOTE: Bracketed numbers are derived from Equations 15, 16, and 17. Underlined numbers are from Equations 18, 19 and 20 based on Section 21 WF 62 values.

$$M_y = Z_x \sigma_y \quad (15)$$

$$R = r \quad (16)$$

$$\phi_y = \frac{2}{y_P + y_E} \epsilon_y \quad (17)$$

where Z_x = the plastic section modulus.

Note that when μ is small the characteristic curvature approaches the lower limiting value of

$$\phi_y = \frac{\epsilon_y}{y_E} \quad (17a)$$

and for large values of μ it approaches the upper limiting value of

$$\phi_y = \frac{\epsilon_y}{y_P} \quad (17b)$$

b) When the moment-curvature parameters are known for a particular section,

$$M_y^{(B)} = \frac{Z_x^{(B)}}{Z_x^{(A)}} M_y^{(A)} \quad (18)$$

$$R^{(B)} = R^{(A)} \quad (19)$$

$$\phi_y^{(B)} = \frac{(y_P + y_E)^{(A)}}{(y_P + y_E)^{(B)}} \phi_y^{(A)} \quad (20)$$

Superscript (A) denotes the particular section for which the moment-curvature parameters are known, and superscript (B) denotes the section for which the parameters are being found. Similar to (a) above, when μ is small the yield curvature approaches

$$\phi_y^{(B)} = \frac{y_E^{(A)}}{y_E^{(B)}} \phi_y^{(A)} \quad (20a)$$

and for large values of μ it approaches

$$\phi_y^{(B)} = \frac{y_P^{(A)}}{y_P^{(B)}} \phi_y^{(A)} \quad (20b)$$

Moment-curvature parameters obtained from Equations (15) to (17) are shown in Tables II through V for comparison. These Tables also show the results of Equations (18) to (20) based on 21 WF 62 values.

ALTERNATE EXPRESSION

For small values of M (compared to M_y) the moment-curvature relation of a section is elastic. The slope of Equation (14) at the origin

$$\frac{dM}{d\phi} = \frac{M_y}{\phi_y}$$

therefore must equal the elastic slope EI (Young's Modulus times moment of inertia) of the section. This gives the relation

$$\phi_y = \frac{1}{EI} M_y \quad (21)$$

Equation (17) may be replaced by Equation (21) if desired. These are shown compared in Figures 8 and 10. For large values of r and μ , Equation (17) results are closer to the actual moment-curvature plot.

DISCUSSION OF RESULTS

The variation in y_P or y_E from the average value $(y_P + y_E)/2$ is found to be between 4.2 and 8.4% for the sections used. See Table 1. Since the actual center of stress y_R is between y_P and y_E the above variation becomes an upper limit for y_R in Equation (12).

Moment-curvature parameters are found somewhat dependent on the curve length (or the ductility ratio μ) employed in curve fitting. This is found to be the case with experimental data as well.

The exponent R approximately equals r of the corresponding stress-strain curve. The difference between them becomes negligible as the ductility ratio increases.

Varying the ductility ratio or the exponent r effects the characteristic moment M_y very little. The latter remains practically unchanged.

Reducing the exponent r or the ductility ratio μ has similar effects on the characteristic curvature parameter ϕ_y .

CONCLUSIONS

A stress-strain relation of the Ramberg-Osgood type across a beam section has been shown to result in a Ramberg-Osgood moment-curvature function for the section.

The plastic section modulus of a cross-sectional area appears to be an important parameter for determining the characteristic moment parameter M_y .

Simple expressions are presented for finding the Ramberg-Osgood moment-curvature parameters for wide-flange sections

- a) from the stress-strain parameters of the material.
- b) from the moment-curvature parameters of a section.

Remarkable agreement exists between these simple expressions and the actual results.

It should be noted in closing that the data available in the literature were not sufficient to allow the experimental verification of the results presented in this paper.

REFERENCES

1. Popov, E. P., and Franklin, H. A., "Steel Beam-to-Column Connections Subjected to Cyclically Reversed Loading," Proceedings, Structural Engineers Association of California, October, 1965.
2. Berg, G. V., "A study of the Earthquake Response of Inelastic Systems," AISI Project 119, Proceedings, Structural Engineers Association of California, October, 1965.
3. Jennings, P. C., "Response of Simple Yielding Structures to Earthquake Excitation," Ph.D. Thesis, California Institute of Technology, June 1963.
4. Hanson, R. D., "Post-Elastic Dynamic Response of Mild Steel Structures," Ph.D. Thesis, California Institute of Technology, June 1965.
5. Morrow, J., "Cyclic Plastic Strain Energy and Fatigue of Metals," ASTM Special Technical Publication No. 378, 1965.

ACKNOWLEDGEMENTS

This paper was developed in connection with earthquake response studies AISI Project 119, Department of Civil Engineering, University of Michigan, Ann Arbor, Michigan.

APPENDIX - NOTATIONS

The following symbols are used in this paper:

b, b' = width of rectangle

c, c' = half depth of rectangle

q = force

q_y = characteristic force

r = an exponent

t = flange thickness

w = web thickness

x = displacement

x_y = characteristic displacement

x_σ = stress

y = distance from the neutral axis

y_E, y_P, y_R = stress center elastic, plastic and Ramberg-Osgood

$z_m = \frac{\sigma_m}{\sigma_y}$ = stress at the extreme fiber of yield stress

EI = Young's modulus times moment of inertia

F = force

M = moment

M_y = characteristic moment

M_A, M_B, M_{WF} = moment

R = an exponent

S_x = section modulus

Z_x = plastic section modulus

$\epsilon, \epsilon_m =$ strain

$\epsilon_y =$ characteristic strain

$\mu = \epsilon_m/\epsilon_y =$ ductility ratio

$\sigma, \sigma_m =$ stress

$\sigma_y =$ characteristic stress

$\phi =$ curvature

$\phi_y =$ characteristic curvature

UNIVERSITY OF MICHIGAN



3 9015 03024 3995